https://doi.org/10.5194/egusphere-2026-221
Preprint. Discussion started: 22 January 2026
© Author(s) 2026. CC BY 4.0 License.

Objective biome classification across global vegetation models reveals consistent biome shifts under future climate change

Simon Scheiter[1,2], Jinfeng Chang[3], Philippe Ciais[4], Marie Dury[5,6], Louis Francois[6], Matthew Forrest[1], Alexandra Henrot[6], Christopher P. O. Reyer[7], Sonia Seneviratne[8], Jörg Steinkamp[9], Wim Thiery[10], Wenfang Xu[11], and Thomas Hickler[1,2]

[1]Senckenberg Biodiversity and Climate Research Centre (SBiK-F), Senckenberganlage 25, 60325 Frankfurt am Main, Germany
[2]Institute of Physical Geography, Goethe University Frankfurt am Main, Altenhoeferallee 1, 60438 Frankfurt am Main, Germany
[3]Zhejiang University, China
[4]Laboratoire des Sciences du Climat et de l'Environnement, LSCE/IPSL, CEA-CNRS-UVSQ, Université Paris-Saclay, F-91198 Gif-sur-Yvette, France
[5]Institut scientifique de service public (ISSeP), Liege, Belgium
[6]Unit for Modelling of Climate and Biogeochemical Cycles, UR-SPHERES, University of Liège, Belgium
[7]Potsdam Institute for Climate Impact Research (PIK), Member of the Leibniz Association, Telegrafenberg, 14473 PotsdamPotsdam, Germany
[8]ETH Zurich, Switzerland
[9]Data Center, Johannes Gutenberg-University Mainz, Anselm-Franz-von-Bentzelweg 12, 55128 Mainz, Germany
[10]Vrije Universiteit Brussel, Department of Water and Climate, Brussels, Belgium
[11]Laboratoire des Sciences du Climat et de l'Environnement, France

Correspondence: Simon Scheiter (simon.scheiter@senckenberg.de)

Abstract. Climate change is altering ecosystems and will reshape the global distribution of biomes. These shifts can significantly influence ecosystem functions and services that are essential for human livelihoods. Robust assessments of future biome dynamics are therefore urgently needed. Here, we employed random forest models and 31 observation-based biome maps representing current land cover to classify outputs from five global vegetation models (GVMs) into biomes, and evaluated potential biome shifts under three climate change scenarios (RCP2.6, RCP6.0, RCP8.5). Model-derived biome maps showed strong agreement with observation-based maps (average κ=0.77), with higher agreement for biomes with well-known temperature constraints. Across all scenarios, GVMs projected biome shifts until the end of the century, where the likelihood of change increased with the level of climate change in RCP scenarios. Between 4% and 56% of the land surface were projected to undergo biome transitions in different combinations of GVMs, RCP and observation-based biome maps used to create biome maps. Broad spatial patterns of biome change were consistent across models. Poleward shifts of boreal and temperate forests dominated, as biomes follow temperature change. Equatorial rainforests remained largely stable, while other studies found forest dieback. These findings highlight regions and biomes most susceptible to future climate change, even under the low-emission scenario RCP2.6. Our transparent and objective biome classification approach can be applied to any vegetation model and provides critical insights for targeted climate mitigation and adaptation strategies and conservation of the remaining natural vegetation.

https://doi.org/10.5194/egusphere-2026-221
Preprint. Discussion started: 22 January 2026
© Author(s) 2026. CC BY 4.0 License.

1 Introduction

Climate change is already affecting ecosystem dynamics, their biogeographic distribution, and thereby the provision of ecosystem services that are essential for human societies (Parmesan et al., 2022). In turn, changes of the land surface can influence climate via biophysical feedbacks (Bonan, 2008). Future climate change is expected to strengthen such impacts, and result, for instance, in drought-induced tree mortality (McDowell et al., 2018), enhanced fire danger (Hetzer et al., 2024), or threats to ecological networks (Schleuning et al., 2016). A robust assessment of potential changes of ecosystem dynamics and ecosystem services is therefore urgently needed to inform conservation and climate change mitigation and adaptation. Biomes, large-scale vegetation formations defined by their functional or structural features (Mucina, 2019), have often been used as units to assess vegetation change. Biomes are typically well associated with the prevailing climatic conditions due to bioclimatic limits such as chilling requirements or frost tolerance (Prentice et al., 1992), as well as with natural disturbance regimes that constrain the spatial distribution of biome-specific species. Biomes have been associated with important ecosystem services such as carbon storage, climate regulation, or biodiversity (Parmesan et al., 2022).

Assessing future biome change is complex, as different drivers of their distributions interact and may have contrasting effects on their distribution. For instance, in tropical savannas, increases in atmospheric CO_2 and CO_2 fertilization of C_3 photosynthesis may enhance woody encroachment and transitions towards woodland and forest (Midgley and Bond, 2015), while increasing drought or changes in fire regimes due to management or changes in fire conditions may counteract woody encroachment (Scheiter and Savadogo, 2016). In boreal forests, warming may enhance growing season length, photosynthetic rates, and forest expansion, which are all strongly controlled by temperature (Lucht et al., 2002). Climate model-derived future projections of temperature changes show more consistent global patterns than those for precipitation changes, which are more uncertain (Shi et al., 2021). Hence, boreal forests and other biomes with clear bioclimatic limits should respond more consistently to climate change than biomes primarily limited by moisture or disturbances, or those without clear bioclimatic limits. In addition to climate, land use and management have substantially transformed biome patterns, and a large proportion of the land surface is covered by non-natural biomes (Fischer et al., 2022). Direct anthropogenic impacts, such as transformation into cropland, can override any climate change-induced biome change.

Global vegetation models (GVMs, Prentice et al., 2007) have been used to study the potential impacts of climate change on biome distributions, ranging from the regional (e.g., Scheiter et al., 2018) to the global scale (e.g., Gonzalez et al., 2010). Such comparisons are, however, associated with different sources of uncertainties. GVMs differ in the representation of ecological processes, plant functional types (PFTs) and disturbances such as fire or drought-induced mortality, and how PFTs are parameterized, such that simulations of current vegetation patterns and responses to climate change differ between models (Smith et al., 2014; Sitch et al., 2008). Further, the biome type of a grid cell is typically not a model output variable but derived in a post-processing step. Using model state variables such as leaf area index (LAI) or cover fractions of different PFTs and biome-specific thresholds for those state variables, modeled vegetation is classified into different biomes. For instance, in a classification scheme typically used for LPJ-GUESS, a tree LAI above 2.5 and dominance of the tropical evergreen tree PFT represent tropical rainforest (Hickler et al., 2012), and in aDGVM, tree cover of more than 80% is typically categorized as

https://doi.org/10.5194/egusphere-2026-221
Preprint. Discussion started: 22 January 2026
© Author(s) 2026. CC BY 4.0 License.

forest (Martens et al., 2021). Model variables, thresholds and biome types used in different studies and GVMs are commonly not unique and to some extent arbitrary, and may differ between studies. This makes objective and direct comparisons of modeled biome patterns and biome change difficult. Dallmeyer et al. (2019) therefore harmonized functional types and biomes to enable comparisons of modeled biome distributions, and Champreux et al. (2024) proposed a method to aggregate biome types to allow comparisons of biome schemes with different numbers of biome types.

A further caveat for analyzing modeled biome distributions and to evaluate models based on observation-based biome maps is that multiple observation-based biome or land cover maps were developed (see Beierkuhnlein and Fischer, 2021; Fischer et al., 2022, for overview). These maps differ in the quantities used for classification, such as species distributions, climate or various remote sensing products, in the number and definition of biome types included in the maps, and their spatial patterns. Champreux et al. (2024) showed that disagreement between biome maps is generally highest in areas with moderate vegetation cover and strong anthropogenic impacts. The biome classification scheme applied to GVM results and the observation-based biome map used for data-model comparisons can therefore influence data-model agreement and projected rates of biome shifts under future climate conditions (Scheiter et al., 2024a). Misclassification of biomes may result in inappropriate conclusions for conservation and management policies for ecosystems (Kumar et al., 2020).

These uncertainties and caveats make it difficult to provide an objective comparison of potential biome change across different GVMs. To mitigate this, we used machine learning (random forests) for a reproducible and objective biome classification based on the LAI distribution simulated by five GVMs and 31 observation-based biome maps provided by Fischer et al. (2022). All GVMs were run following the protocol of the Inter-Sectoral Impact Model Intercomparison Project phase 2b (ISIMIP2b) using the same environmental forcings (Frieler et al., 2017) and fire enabled, but correcting for anthropogenic land use to represent natural vegetation biomes. We applied supervised classification to classify annual LAI of different PFTs simulated by the GVMs under current conditions (2006 to 2020) into each of the 31 biome maps. Even though a variety of variables such as vegetation cover, vegetation height or productivity is available for the GVMs and suitable for biome classification, we only selected LAI. This variable is directly simulated by GVMs, observable globally, and it is a core biophysical variable in GVMs, linked to canopy structure, light availability and productivity. It has also been used for biome classification in GVMs (e.g., Smith et al., 2014) and our analyses are therefore consistent with previous studies. Then, we assessed the agreement between all combinations of GVM- and observation-based biome maps, and agreement of potential biome change until the end of the century (2085-2099) under three climate change scenarios (RCP2.6, 6.0 and 8.5) to identify the areas with biome stability and areas most susceptible to biome change. In addition to GVM results, we applied random forest models to classify observation-based PFT maps into biomes (Tuanmu and Jetz, 2014; Harper et al., 2023), and we compared the performance of classifications based on GVMs and observation-based PFT maps.

We hypothesize that (1) observation-based biome maps can be reproduced using GVM results, but agreement between modeled and observation-based biome maps (quantified by κ statistics) shows large variation between GVMs and biome maps used to inform biome classification; (2) accordingly, the extent of biome change until the end of the century differs between GVMs, while the broad spatial patterns of biome stability and susceptibility to biome change are consistent between models, (3) model performance (i.e., κ statistics) is better for biomes where the boundaries are largely driven by relatively well-understood

https://doi.org/10.5194/egusphere-2026-221
Preprint. Discussion started: 22 January 2026
© Author(s) 2026. CC BY 4.0 License.

temperature limits, because temperature-related bioclimatic limits in the models constrain the extent of PFTs and accordingly of biomes, and (4) future projections are more consistent for biomes with temperature limits, because of the robust trends of temperature change in the climate change scenarios used in our analysis.

2 Methods

2.1 Data

GVM simulation results were obtained from the ISIMIP repository (data.isimip.org, see Table S1 for summary of all data sets used for the analysis). Specifically, we used simulation results from ISIMIP2b simulations for the climate change scenarios RCP2.6, RCP6.0, and RCP8.5, simulated with climate forcings from IPSL-CM5A-LR or HADGEM2-ES Earth System Models (ESMs, Frieler et al., 2017; Reyer et al., 2024). Both climate forcing data sets were bias corrected with EWEMBI observational data (Lange, 2018, 2019). ISIMIP2b simulation runs include different combinations for direct anthropogenic impacts and atmospheric CO_2 (increasing or fixed). Here, we used the scenario where land use, nitrogen deposition and fertilizer input was included but fixed at the levels of the year 2005 ('2005soc' scenario) and where CO_2 increased according to the respective RCP scenario ('co2' scenario). We selected the combination of IPSL-CM5A-LR, '2005soc' and 'co2', because for this combination, results were available for five different GVMs for RCP6.0. Model results were available for LPJ-GUESS (Smith et al., 2014), ORCHIDEE (Guimberteau et al., 2018), ORCHIDEE-DGVM (Guimberteau et al., 2018), CLM4.5 (Thiery et al., 2017), and CARAIB (Minet et al., 2015; Warnant et al., 1994). For RCP2.6 and RCP8.5, we used HADGEM2-ES results for CLM4.5, as results for IPSL-CM5A-LR were not available in the repository. For RCP8.5, results were only available for LPJ-GUESS, ORCHIDEE and CLM4.5. As we did not run model simulations for this study but only used available model results, we do not provide model descriptions or model comparisons and refer to the key references for the different models (Supplement S1).

The target variable for biome classification was leaf area index (LAI), because this variable has historically been used for biome classification (e.g., Hickler et al., 2006; Smith et al., 2014). Using LAI ensures consistency with previous studies. For our analyses, we only used PFTs representing natural vegetation while bare ground and anthropogenic PFTs were ignored (see Supplement S1 for details). Annual LAI data were averaged for the 15-year periods 2006-2020 and 2085-2099, representing early and late conditions within the future simulations of ISIMIP2b that were provided for the period 2006-2099 for each climate scenario. Climate conditions in different RCPs do not differ strongly for the early period (2006-2020) but diverge only after that period. Therefore, we hereafter denote the early period as 'current' irrespective of the RCP scenario, and the late period as 'future'. LAI data in the ISIMIP repository did not account for cover fractions of different PFTs within grid cells. Therefore, we processed LAI data in two steps. First, we multiplied PFT-specific LAI with the cover fraction of the respective PFT. Then, we scaled the LAI of natural PFTs with the inverse sum of the cover fractions of all natural PFTs. The second scaling step removes anthropogenic PFTs and assumes that the entire grid cell is only covered by natural PFTs (see Supplement S1 natural/anthropogenic PFTs). This scaling is reasonable, as we only consider natural biome types in our biome classification (see section 'Biome classification'). The data were available at 0.5° spatial resolution.

https://doi.org/10.5194/egusphere-2026-221
Preprint. Discussion started: 22 January 2026
© Author(s) 2026. CC BY 4.0 License.

We used 31 biome maps compiled by Fischer et al. (2022), hereafter called F31 biome maps. Those maps were published between 1964 (Walter, 1964, with adjustments and revisions afterwards) and 2020 (Allen et al., 2020), and therefore represent current and historic biome patterns. We ignored potential biome shifts after the publication of biome maps and compared all maps to the model results for current conditions (2006-2020). The biome maps were derived from different quantities and by different methods, such as biogeographic mapping of species, bioclimatic zonation or classification using remote sensing data. Hence, the biome maps represent different functional and structural features of vegetation. The maps differ substantially with respect to the number of biomes included, the definition of different biome types, and accordingly their spatial distributions. As GVM results from the ISIMIP2b repository were provided at 0.5° spatial resolution (see previous paragraph), we aggregated the biome maps to the same 0.5° resolution using the nearest neighbor method.

In addition to GVM results, we used observation-based PFT maps for our analysis: the European Space Agency (ESA) Climate Change initiative (CCI) product (Harper et al., 2023) and the Tuanmu and Jetz (2014) product. The products include different sets of PFTs (supplement S1). Those PFT maps were derived from different remote sensing products. Harper et al. (2023) developed a cross-walking scheme to match PFT distributions with land cover classes from the CCI Multi-Resolution Land Characteristics (MRLC) product, supported by products describing for example surface water, built-up areas or tree canopy cover and height. Tuanmu and Jetz (2014) used classification and data integration approaches to create a consensus map based on reflectance data from GlobCover Land Cover (GlobCover), Moderate Resolution Imaging Spectroradiometer (MODIS2005), Global Land Cover 2000 (GLC2000) and IGBP Data (DISCover). Even though those products are observation-based, they are expert-based and subjective and affected by uncertainties (Wang et al., 2023). Classification with those products serves as reference for the evaluation of GVM results; future changes of PFT maps are not available. Both products were aggregated to the 0.5° spatial resolution of the GVM results using bilinear interpolation.

2.2 Biome classification

We used random forests to classify PFT information from GVMs (based on LAI) or remote sensing (cover fraction) into the F31 observation-based biomes, that is, we applied supervised classification. For each combination of one of the F31 biome maps, modeled LAI or observation-based PFT cover map, and RCP scenario, one random forest model was created. Simulated LAI for current conditions or cover fractions were used as explanatory variables, the biome types of the respective biome maps were used as response variables, where all biome types were classified in one random forest model. For each random forest, 2500 trees were created. Using the random forests, we then predicted biome patterns for current conditions for each GVM or PFT map and for each of the F31 biome maps. Overall, we created 62 biome maps for PFT products (31 biome maps, 2 PFT products), 155 maps for five GVMs for RCP2.6 and RCP6.0, and 93 maps for three GVMs for RCP8.5. We further applied the random forest models to the PFT-specific LAI simulated by GVMs for future (period 2085-2099) climate and CO_2 conditions of the respective GVM, to obtain biome patterns for future conditions. This was only possible for the five GVMs, as future projections for the PFT cover products were not available. Random forests were fitted using the 'randomForest' R package (Liaw and Wiener, 2002).

https://doi.org/10.5194/egusphere-2026-221
Preprint. Discussion started: 22 January 2026
© Author(s) 2026. CC BY 4.0 License.

2.3 Analyses

For comparisons between observation-based biome maps (Fischer et al., 2022) and the biome patterns obtained from random forest models trained on the respective biome maps, we used the κ-statistics (Monserud and Leemans, 1992). This quantity allows comparisons between the spatial patterns of categorical variables and considers that agreement can be caused by random effects. Values in the range 0-0.2 indicate slight agreement, 0.2-0.4 fair, 0.4-0.6 moderate, 0.6-0.8 substantial and 0.8-1 almost perfect agreement. We created maps to identify areas where the F31 and respective modeled biome maps agree or disagree, and assessed the relationship between κ values and the number of biomes in the respective biome map. We assumed that the entire 0.5° grid cell is covered by only one biome type, both in the F31 maps and the model results. For these analyses of model performance under current climate conditions, we present only results from the RCP6.0 scenario, as vegetation simulations for the current period and agreement with observation-based biome maps are similar.

For the GVM results, we analyzed the susceptibility to biome change under future climate and CO_2 conditions and regions of biome stability. Therefore, we created maps indicating biome change or stability between current and future climate conditions for each GVM and for each of the F31 biome maps. Hence, we obtained 155 maps of biome change (5 GVM $\times$ 31 biome maps) for RCP2.6 and RCP6.0 and 93 maps for RCP8.5. These maps were then overlaid and the number of models projecting a biome change was counted. Values approaching 155 or 93 indicate that all models consistently predict biome change whereas low values indicate that models consistently predict biome stability. We denote the number of models projecting biome change as the susceptibility of biome change. A high number of GVM-biome-map projecting a biome change in a grid cell is associated with a high susceptibility of biome change. To visualize this, we categorized these results into categories, where 'low' indicates that 0 to 20% of the models indicate a biome change, 'Medium' indicates 20 to 40%, 'high' indicates 40 to 60% and 'very high' more than 60%. We assessed if the proportion of grid cells affected by biome change is related to the agreement between data and model results (i.e., to the κ value) or to the number of biomes in the respective biome map. We used a linear regression to test if the number of grid cells affected by biome changes can be explained by the RCP scenario, GVM, F31 biome map, and number of biomes in the biome map.

2.4 Olson et al. (2001) map as an example

To exemplify modeled biome distributions and biome change, we analyzed the results for the Olson et al. (2001) biome map in more detail. We selected this map as it is commonly used as reference biome map, for example in IPBES or in biome-specific analyses (e.g., Sanderson et al., 2002; Loarie et al., 2009; Newbold et al., 2016). We created maps showing the current and future biome patterns, agreement between modeled and observation-based biome distributions, as well as maps indicating regions where biome shifts occur. To quantify the agreement per biome, we calculated contingency tables for each model indicating the percentages of overlap between observation-based and modeled biomes. In addition, κ values were calculated per biome by setting grid cells covered by the target biome to one and all other biomes to zero, and then calculating the κ value for the binary map. We created Sankey plots to illustrate transitions between biomes between current and future conditions

https://doi.org/10.5194/egusphere-2026-221
Preprint. Discussion started: 22 January 2026
© Author(s) 2026. CC BY 4.0 License.

using the 'ggsankey' package (Sjoberg, 2024), and quantified biome coverage and transition rates for current and future biome distributions.

To test if agreement between modeled biomes for current conditions and the Olson et al. (2001) biomes is higher for temperature-driven biomes, we first split the biome types into those mainly driven by temperature and those driven by other factors (Table S2). This classification is based on literature and expert-knowledge, and other authors may use another classification. Then, we calculated the mean κ values for both groups and all GVM and PFT maps. To test if the likelihood of biome change differs between biomes mainly constrained by temperature or other factors, we calculated the percent of grid cells predicted to undergo biome change for both groups.

To test if biome change is more consistent for biomes with well-defined temperature limits such as chilling requirements or frost tolerance used to define PFTs, we used the coefficient of variation as proxy for consistency. Specifically, we calculated for each GVM and each biome transition the respective percent of grid cells affected by this biome change. Then we calculated mean, standard deviation, and coefficient of variation of these percentages for each biome change across the GVMs. To account only for relevant biome change, we excluded those with less than 5% coverage under current conditions. Finally, we used a t-test to compare mean coefficient of variation for biomes with well-defined temperature limits and biomes explained by other factors. If biome change for temperature-defined biomes are more consistent, we would expect lower coefficients of variation.

All analyses were conducted using R (R Core Team, 2024). Spatial data were processed using the 'terra' (Hijmans, 2024) package. Figures were created using the 'ggplot2' (Wickham, 2016) package.

3 Results

3.1 Biome classification

Data-model agreement varied strongly across the 31 biome maps (Fischer et al., 2022) and different LAI or PFT data used for the biome classification (Fig. 1). Overall, κ values were higher for biome classification using observation-based PFT data (mean $\kappa = 0.95$, indicating almost perfect agreement) than for LAI data simulated by GVMs (mean $\kappa = 0.77$, indicating substantial agreement). Of the F31 biome maps used to inform the biome classification, agreement was highest for the Schultz (2016) biome map when averaging κ for all GVMs ($\kappa = 0.83$), for the The Nature Conservancy (2009) map for GVMs and PFT maps combined ($\kappa = 0.87$), and for the Buchhorn et al. (2020) biome map for classification using only the observation-based PFT maps ($\kappa = 0.98$). The lowest overall performance was obtained for the Tateishi et al. (2011, 2014) map ($\kappa = 0.75$). The relation between the κ values and the number of biomes included in the F31 biome maps was weak (Fig. S1, Table S3).

Regions where observation-based and modeled biomes agree or disagree were spatially heterogeneous (Fig. S2), and discrepancies were generally higher at biome boundaries (not shown). Agreement was high, for example, in Northern Europe, Northern America, and tropical forest regions in Brazil or Southeast Asia (Fig. S2). Agreement was low in on the Tibetan plateau, a large part of the sub-tropics in South America or regions bordering the central African rainforests. Those spatial patterns differed between GVMs and observation-based PFT maps (Fig. S2). For instance, CARAIB showed the highest

https://doi.org/10.5194/egusphere-2026-221
Preprint. Discussion started: 22 January 2026
© Author(s) 2026. CC BY 4.0 License.

disagreement in northern latitudes and around the Equator, whereas ORCHIDEE-DGVM showed highest disagreement in sub-tropical regions bordering equatorial forests.

3.2 Biome shifts under climate change

The proportion of grid cells projected to be affected by biome change increased from RCP2.6 to RCP6.0 but was lower in RCP8.5 than in RCP6.0. The RCP8.5 scenario lacks CARAIB and ORCHIDEE-DGVM simulations, the two models with the highest rate of biome shift in other RCP scenarios. In addition to the proportion of grid cells, the susceptibility category increased, indicating higher consensus between different models (Fig. 2). Thus, the area affected by low susceptibility changed from 53.1% in RCP2.6 to 32.8% in RCP6.0 and 40.1% RCP8.5, while the proportion of grid cells affected by high or very high susceptibility increased from 3.6% in RCP2.6 to 15.5% in RCP6.0 and 10.7% in RCP8.5. Yet, the broad spatial pattern of regions affected by biome change were similar for different RCPs (Fig. 2). For instance, the tropical forests of Africa and Southeast Asia were projected to be stable in all scenarios while northern latitudes or southern Africa showed a susceptibility of biome change in all RCPs. The spatial patterns of biome change also differed between GVMs (Fig. S3).

For all combinations of the GVMs and F31 biome maps, the proportion of the grid cells affected by biome change ranged between 4 - 45% for RCP2.6, 7 - 56% for RCP6.0, and 9 - 53% for RCP8.5 (Figs. 3, S4). When averaged across all F31 biome maps for each GVM and each RCP, the proportion of grid cells affected by biome change was lowest for CLM4.5 for all RCPs (4.2, 6.6 and 9.3%) and highest for CARAIB and ORCHIDEE-DGVM for RCP2.6 (44.5%), CARAIB for RCP6.0 (56.3%) and LPJ-GUESS for RCP8.5 (52.7%, with CARAIB and ORCHIDEE-DGVM not being available for RCP8.5). The proportion affected by biome shifts was related to data-model agreement (i.e., the κ value of the respective model, Figs. 3, Table S4). Considering each GVM individually, the proportion decreased with κ, that is, higher data-model agreement implied a lower rate of biome shifts. When considering all models together, the proportion increased with κ, and the model with the highest overall performance (CARAIB) showed the highest proportion of biome shifts (Fig. 3, S4). These relations were consistent for all RCPs (Fig S4). The relation between the rate of biome shifts and the number of biomes in the biome map was positive but weak (Figs. 3, S4, Table S5), i.e., more biome types in the biome map imply a higher proportion of biome change. Yet, some biome maps with a lower number of biomes also showed high proportions of biome change.

The regression model showed, that the RCP scenario had a highly significant effect on the number of grid cells affected by biome change (t statistics <0.001). The effects of the F31 biome map, GVM and the number of biomes in the map had significant effects (t statistics between 0.01 and 0.05).

3.3 Comparison with Olson et al. (2001) biomes

Our biome classification with random forests reproduced the Olson et al. (2001) biome map with high agreement. The κ value ranged between 0.69 for random forests informed by CLM4.5 and 0.99 for models informed by Tuanmu and Jetz (2014), indicating substantial to almost perfect agreement (Tables S8 to S14). Biome-specific κ varied largely within models and for biomes between different models. For example, the values ranged between 0.40 (moderate agreement) and 0.91 (almost perfect agreement) for different biomes in ORCHIDEE, and between 0.1 (slight agreement) and 0.96 for ‘flooded grassland and

https://doi.org/10.5194/egusphere-2026-221
Preprint. Discussion started: 22 January 2026
© Author(s) 2026. CC BY 4.0 License.

savanna' between different GVMs (and 0.99 for the Tuanmu and Jetz (2014) data). While the proportion of grid cells with data-model disagreement differed between the models, the regions overlapped substantially (Fig. S5). For example, disagreement occurred in areas bordering the central African rainforests, India or the west of North America where temperate conifer forest was not captured by some of the models (Fig. S5). Apart from the CARAIB model, κ values were higher for biomes with biome boundaries controlled by temperature, compared to biomes controlled by other factors (Table 1). Yet, differences were not significant.

The five GVMs projected substantial biome transitions until the end of the century (Fig. 5). The proportion of grid cells where all models projected biome shifts were 0.1, 0.3 and 1.4% of the land surface for RCP2.6, RCP6.0 and RCP8.5, while the proportion of grid cells not affected by biome change in any model were 51.6, 38.7 and 47.9% for the RCPs. For RCP6.0, the percent of grid cells affected by biome shifts ranged between 6.8% for CLM4.5 and 37.1% for CARAIB. The regions affected by biome change did not fully match, but we identified hotspots of potential biome shift. Regions where models consistently simulated biome transitions were scattered across different continents and biomes, for example along the 'boreal forest' - 'temperate broad-leaved mixed forest' biome boundary or in the south of Brazil (Fig. S6). Further, most models projected transitions towards 'tropical mixed broad-leafed forest' in the regions bordering the central African rainforests, or transitions to 'tropical grassland savanna and shrub' in India.

When considering all GVMs and RCPs, the most frequent biome transition was from 'tropical and subtropical dry broadleaf forest' to 'tropical and subtropical grassland savanna and shrubland' (43.0%, 52.4% and 52.9% of grid cells affected by change for RCP2.6, RCP6.0 and RCP8.5, respectively, Fig S8). Yet, coverage of 'tropical and subtropical dry broadleaf forest' is low under current conditions. When considering only biomes with more than 5% coverage under current conditions, the most frequent transitions were modeled between 'tundra' and 'boreal forest/taiga' (18.1, 27.8 and 18.2% affected, Fig 6, Table S6). As hypothesized, the analyses showed that biome change was slightly more consistent for temperature-controlled biomes then for other biomes, but not significant (coefficient of variation 0.61 for temperature-driven biomes and 0.68 for others in RCP6.0, p-value 0.522), even though the proportion of grid cells affected by change was smaller for temperature-driven biomes (Table 2).

4 Discussion

We used LAI simulated by five different GVMs and random forest classification to classify GVM results into biomes of 31 different biome maps (Fischer et al., 2022). In contrast to previous studies using model-specific, expert-based classification schemes, our approach is objective and based on multiple biome and land cover maps. This approach facilitates direct comparisons of current and future biome pattern between a large number of model projections. We showed that observation-based biome maps can be reproduced with high agreement, particularly for biomes constrained by well-known temperature limits. Biome changes were modeled with all GVMs for three different RCP scenarios, and the broad spatial patterns of regions susceptible to biome change agreed. Those regions were scattered across all continents. Overall, poleward shifts of biomes were evident, following temperature increases.

https://doi.org/10.5194/egusphere-2026-221
Preprint. Discussion started: 22 January 2026
© Author(s) 2026. CC BY 4.0 License.

4.1 Biome classification for current conditions

As expected, random forest models using GVM results and observation-based PFT maps showed high performance and agreement with the F31 biome maps (high κ value). The performance of RFs using PFT maps was higher than those using GVM results. This result is, however, not surprising as PFT maps were derived from various remote sensing products (Tuanmu and Jetz, 2014; Harper et al., 2023), and they are therefore not fully independent from biome maps derived from similar remote sensing products (Fischer et al., 2022). It is more remarkable that biome maps derived from GVM results showed high agreement with observation-based biome maps ($\kappa > 0.8$) for some combinations of GVM and the F31 biome maps. GVMs are process-based and bottom-up (Prentice et al., 2007), and biome information is typically not directly used to parameterize such models. Yet, some models constrain current and future PFT cover fractions (e.g., CLM4.5) using observation-based PFT or biome data, instead of simulating PFT cover dynamically (e.g., LPJ-GUESS). However, LPJ-GUESS and other models use bioclimatic limits to constrain the distribution of PFTs, and these constraints also influence the possible distributions of biomes defined by those PFTs.

For GVMs, κ values were highest for the Schultz (2016) biome map. Classification in this map is based on vegetation, climate and other environmental factors, and re-evaluation of previous, regional-scale studies. The Schultz (2016) map shows a clear arrangement of biomes along environmental gradients and the relation to climatic drivers. High agreement with GVM results illustrates that biomes simulated by GVMs reflect the prevailing climatic conditions and bioclimatic limits that constrain the distribution of PFTs. Similarly, agreement between GVMs and the Olson et al. (2001) map, a map derived from species distributions and biogeographic zonation, was high. The Olson et al. (2001) map has often been used as reference map in biome-specific studies, for example, of the human footprint (Sanderson et al., 2002), climate change velocity (Loarie et al., 2009), or biodiversity intactness (Newbold et al., 2016). High agreement confirms that the Olson et al. (2001) biome map is suitable as a reference for such analyses.

Agreement between observation-based and modeled biomes was spatially heterogeneous. In the Olson et al. (2001) map, agreement was lowest on the Tibetan plateau. This region is classified as 'montane grassland and shrubland' in the Olson et al. (2001) map, whereas GVMs simulated mixtures of 'montane grassland and shrubland' or 'tundra'. While both biomes are characterized by cold temperature, 'montane grassland and shrubland' in the Olson et al. (2001) map occurs only in high altitudes; this variable is not captured in GVMs and our analysis. Other regions with low agreement were the sub-tropics surrounding the central African rain forests. It has been hypothesized, that in some of these regions, alternative biome states are possible (Pausas and Bond, 2020), that is, depending on fire activity or herbivores, closed forests or open savanna states are possible (Higgins and Scheiter, 2012; Midgley and Bond, 2015). Fire has been included in many GVMs (Hantson et al., 2016), including the models in our study, and shown to influence modeled tree cover and the carbon cycle (Lasslop et al., 2020). If fire enables alternative states and influences biome patterns in our results remains to be tested.

Despite the large variation between different combinations of GVMs and F31 biome maps, κ values were overall higher than in previous studies. For instance, Dallmeyer et al. (2019) reports values between 0.2 and 0.79 in a comparison between different models and classification methods, and Scheiter et al. (2024a) reports a maximum value of $\kappa = 0.52$ for a classification using

https://doi.org/10.5194/egusphere-2026-221
Preprint. Discussion started: 22 January 2026
© Author(s) 2026. CC BY 4.0 License.

functional traits modeled by the aDGVM2. This can be attributed to the application of random forest classification that often shows high performance (Fernandez-Delgado et al., 2014), while previous GVM studies typically applied expert-based biome classification approaches. Random forests maximize the agreement between modeled and observation-based biomes at the expense of clear and justifiable rules to separate between biomes.

4.2 Biome shifts under climate change

All GVMs projected biome shifts until the end of the century, irrespective of the Fischer et al. (2022) biome map used to inform the biome classification. Yet, the proportion of grid cells affected by biome change varied between different RCPs, GVMs and biome maps. Across all RCPs and GVMs, regions with high susceptibility of biome change were distributed on all continents, for example in southern Africa, the northern latitudes of Eurasia, or south of the Amazon rainforests. Biome stability or low susceptibility of biome change was consistently modeled in deserts and tropical rainforests globally. The boundaries of those biomes are primarily constrained by very low or very high precipitation, and projected future precipitation change in the RCP scenarios and the selected ESM is not sufficient to cross these constraints and trigger biome transitions.

Our results confirm previous modeling results. In a global study, Gonzalez et al. (2010) also identified deserts and tropical forests as biomes with lowest susceptibility of biome change but higher susceptibility in the northern latitudes. Huntley et al. (2016) showed with LPJ-GUESS simulations, that a large proportion of desert and rainforest have also been stable during the last 140 ka, showing their stability under past, current and future conditions (at least without direct human impacts). Yet, Parry et al. (2022) found that five out of seven climate-vegetation models project Amazon forest dieback at the local scale, that may, at larger scale, be compensated by increases in carbon elsewhere. Doughty et al. (2023) found that under future warming, tropical forests may approach ecophysiological limits, particularly under RCP6.0 and RCP8.5. However, such effects may be compensated by adaptation and acclimation of temperature optima (Choury et al., 2022). Chambers et al. (2025) found that Amazon forests may experience more hot droughts and non-analogue climate under future conditions, enhancing the risk of forest dieback.

Bonannella et al. (2023) used machine learning approaches to project future biome patterns. While some of the regions affected by biome change agree with our results, for instance regions south of the Amazon and central African rainforests, the area affected by biome change was lower in Bonannella et al. (2023). In addition, Bonannella et al. (2023) projected transitions from tropical forest to savanna in those regions, which can be attributed to the absence of CO_2 fertilization and fire in their approach. Conradi et al. (2024) used a species-based modeling approach and showed that between 33 and 68% of the land surface will undergo change in phyto-climate, that is the climate conditions supporting characteristic plant growth forms, in RCP2.6 and RCP8.5 until 2070. Associated change phyto-climatic zones occurred in temperate, boreal and polar regions, while tropical zones were less likely to change. Using a trait-based modeling approach, Boonman et al. (2022) also showed that boreal forest and tundra are most susceptible to climate change, whereas (sub-)tropical biomes will expand.

For the Olson et al. (2001) biome map, our results indicate that ‘temperate grassland savanna and shrubland’, ‘tundra’ and ‘tropical and subtropical grassland savanna and shrubland’ were most susceptible to biome shifts in all RCPs. This result partly agrees with Gonzalez et al. (2010), who identified temperate mixed forests, boreal conifer forests, and tundra/alpine

https://doi.org/10.5194/egusphere-2026-221
Preprint. Discussion started: 22 January 2026
© Author(s) 2026. CC BY 4.0 License.

as most vulnerable to biome shifts. Similarly, Tobian et al. (2024) showed with the LPJmL model that boreal forests are highly susceptible to dieback while temperate forests are relatively resilient and tropical forests are relatively stable. For the RCP6.0 scenario, between 22% and 51% of the land surfaces is susceptible to biome change for different GVM-biome map combinations in our analysis. This range overlaps with Gonzalez et al. (2010) who estimated that 10 to 50% of the land surface may be vulnerable to biome change by the end of the century.

One reason for discrepancies between our and previous results is that predicted future large-scale dieback events are climate- and vegetation-model-specific (e.g., Sitch et al., 2008; Rammig et al., 2010). For example, LPJ-GUESS in this study did not include the high temperature stress function that LPJmL includes (Tobian et al., 2024) and, therefore, does not predict heat-related mortality and dieback in the boreal forest. Which model combination is most realistic is, at present, impossible to say, partly because it has hardly been tested to what extent the current GVMs can reproduce recent increases in drought- and heat-related tree mortality and extreme fires, e.g., the record fires in Canada in 2023 (MacCarthy et al., 2024). Data-model comparisons for the recent sharp increase in drought-induced mortality of Norway spruce in Central Europe, in some regions reaching 50% of the forest area, have shown that most GVMs fail to reproduce the observed large-scale forest die-back (Anders et al., 2025; Fischer et al., 2025). Thus, the current GVMs might underestimate future risks of climate-induced forest dieback and associated biome shifts, but more studies will be necessary to corroborate such a conclusion.

For each GVM, the proportion of grid cells affected by future biome change decreased as data-model agreement (the κ value) with one of the 31 biome maps (Fischer et al., 2022) increased, i.e., higher agreement implies a lower proportion of grid cells affected by biome change. A similar relation was found in Scheiter et al. (2024a) for the classification of aDGVM2 results into biomes using PFT cover fractions or patterns of functional traits modeled by the aDGVM2 (Scheiter et al., 2013; Langan et al., 2025). This result suggests that the rate of projected biome shifts may be overestimated when a biome classification with low data-model agreement is used. In contrast, biome classifications with high agreement may provide an estimate of the minimum rate of biome change, and potentially a more reliable trend of biome change. For RCP6.0, this lower limit is between 21.9% and 28.9% for the different GVMs.

Interestingly, assessing this relation across all GVMs included in our analysis showed the opposite, i.e., an increasing proportion of grid cells affected by biome change with higher data-model agreement. For better performing GVMs (i.e., higher κ) the random forest is more precisely defined and therefore more sensitive to changes. Biome maps with low performance (i.e., poorer κ values) reflect weaker compatibility with the model PFTs, leading to spurious relationships and reduced sensitivity of the random forest models to LAI changes. CARAIB has the highest number of PFTs and the highest number of grid cells affected by biome change. A biome type may, in our classification, be represented by multiple PFTs, and moderate LAI changes of multiple PFTs may translate into a biome change. In models with a low number of PFTs, such as CLM4.5, a biome can be represented by a single PFT, and substantial changes in LAI may be required to trigger a biome change. In addition, PFT cover fractions in CLM4.5 remain static under future climates, such that biome change is constrained and only driven by LAI change.

https://doi.org/10.5194/egusphere-2026-221
Preprint. Discussion started: 22 January 2026
© Author(s) 2026. CC BY 4.0 License.

4.3 Biome shifts of temperature-driven biomes

Our results support the hypothesis that biomes with well-described temperature limits, including for example tundra and boreal forest (Table S2), are better reproduced by the random forest models than biomes driven by other factors. Yet, differences between κ values of those groups of biomes were not statistically significant. Many GVMs include bioclimatic limits related to temperature to constrain the distribution of different PFT (e.g., Sitch et al., 2003). These limits describe, for example, cold tolerance or chilling requirements of PFTs, and they are based on empirical evidence (Prentice et al., 1992). Given the constraints on PFTs, bioclimatic limits also constrain the distribution of biomes.

Temperature-driven biomes showed lower proportions of grid cells affected by biome shifts than those controlled mainly by other factors. Yet, as expected, biome transitions were slightly more consistent for temperature-driven biomes (not statistically significant), i.e., the variability of specific biome transitions between different models was lower. This could be attributed to the representation of PFTs and bioclimatic limits in the models, but also to spatial patterns of changes in environmental conditions. Temperature is less variable among the climate models than other variables such as precipitation or aridity, and temperature changes are mainly directed poleward, in contrast to other variables (Shi et al., 2021). In the GVMs, temperature increases and elevated CO_2 in different RCP scenarios do not only modify ecophysiological processes, the carbon balance and competitive hierarchies of PFTs but temperature change may also imply that bioclimatic limits of PFTs are crossed. Hence, climatic conditions may become unsuitable for the PFT, which implies poleward biome shifts, following the warming trends in the RCP scenarios. Change in biomes that are not mainly driven by temperature indicate that effects of other variables such as change in rainfall regimes, CO_2 or fire activity have stronger effects on those biomes than change in temperature. Fire is included in many GVMs (Hantson et al., 2016), including models used in our study. A recent analysis highlights the model's applicability for burned area attribution (Burton et al., 2024) and further model comparisons focusing on fire are ongoing (Burton et al., 2025). Yet, we did not analyze fire effects on biome change.

4.4 Limitations and future directions

The LPJ-GUESS version used in this study and some of the F31 biome maps (e.g., Olson et al., 2001) only include natural vegetation, while other GVMs and biome maps also include cultivated areas. For consistency, we used only PFTs and biomes representing potential natural vegetation. Yet, direct human impacts such as deforestation of Amazon rainforests or intense livestock grazing in savannas have shaped the current biome distribution and can accelerate or inhibit biome change in the future (Scheiter and Savadogo, 2016). While land use, nitrogen deposition and fertilizer input were considered but fixed at year 2005 levels in our analysis, it could be repeated by including PFTs and biomes representing cultivated land and by using available ISIMIP results considering changes in land use, nitrogen deposition and fertilizer input according to HYDE3.2 for historic conditions (Klein Goldewijk et al., 2017) and to MAgPIE simulations for SSP2 for future conditions (Popp et al., 2014; Stevanović et al., 2016). Considering only potential natural vegetation is, however, important for conservation and protection of the remaining natural vegetation.

https://doi.org/10.5194/egusphere-2026-221
Preprint. Discussion started: 22 January 2026
© Author(s) 2026. CC BY 4.0 License.

We used LAI simulated by different GVMs for biome classification, for consistency with biome classification schemes used in previous modeling studies (e.g., Smith et al., 2014). LAI is directly modeled by GVM, observable and it has direct biophysical meaning. Our approach provides a functional description of biomes, based on productivity and relative abundance of different PFTs. Thus, boreal or tropical forests are represented by single PFTs with high LAI, while savannas can be represented by a mixture of grasses and trees with intermediate LAI. Other model variables such as biomass, productivity, vegetation height or functional traits are available for biome classification and may improve data-model agreement for some of the F31 biome maps. Yet, using different variables makes our classification less transparent.

Selection of appropriate variables for biome classification is not only relevant for model results but also for observation-based biome maps. Depending on the variables used for classification and the number of biome types represented, the resulting biome maps can vary substantially (Beierkuhnlein and Fischer, 2021; Fischer et al., 2022), and direct comparisons of their agreement would require harmonization and re-classification. Champreux et al. (2024) showed that disagreement between biome maps is generally highest in regions with moderate vegetation cover and anthropogenic impacts. The F31 biome maps span six decades and various mapping approaches, from pre-satellite expert-based maps to modern products that integrate satellite remote sensing products. More recent maps likely have higher spatial precision and better documented validation, especially for broad structural contrasts.

While our random forest classification approach is objective and can be applied to any GVM, it has a major caveat: rules for classification are less transparent than in expert-based biome schemes tailored for specific GVMs and biome types. Yet, identifying thresholds to delineate between biomes using quantitative methods or expert knowledge has their own flaws. We therefore argue, that large-scale model comparisons benefit from utilizing objective classification methods that can be applied to any set of PFTs included in GVMs. Expert-based classification schemes are more applicable for studies with single GVMs.

Vegetation change has been shown to lag behind change in environmental forcings (e.g., Bertrand et al., 2016; Scheiter et al., 2020; Zani et al., 2024). Hence, vegetation and biome patterns are committed to further change to reach an equilibrium state with climate, even if the climate system stabilizes. These lags can be explained by various processes including dispersal limitation, delayed responses of ecological process such as ecophysiology, establishment and mortality, succession, and disturbances such as drought or fire. Dispersal has been integrated into GVMs (e.g., Blanco et al., 2014; Zani et al., 2022). Yet, consideration at global scale is challenging as dispersal is strongly influenced by small-scale processes and heterogeneity that cannot be represented at the 0.5° resolution of the GVM simulations (Lenormand et al., 2009; Snell et al., 2014). Under future climate conditions, tree mortality induced by drought, heat, fire or pests may be enhanced in different regions and biomes (McDowell et al., 2018; Anderegg et al., 2020), but the representation of tree mortality is still limited in vegetation models (Langan et al., 2025; Scheiter et al., 2024b; Anders et al., 2025). Improving the representation of such processes in vegetation models will not only improve the representation of current ecosystem dynamics and biome boundaries, but also reduce uncertainties in projections of future climate change effects.

https://doi.org/10.5194/egusphere-2026-221
Preprint. Discussion started: 22 January 2026
© Author(s) 2026. CC BY 4.0 License.

5 Conclusions

We present an objective biome classification approach that can be applied to any GVM and observation-based biome map, and that allows multi-model comparisons of climate change impacts on future biome distributions. We showed that biome shifts are likely under future climate change scenarios. The most susceptible regions differ between GVMs, RCP scenarios and biome maps used to inform biome classification, highlighting the need for multi-model analyses. Despite these differences, we identified consistent patterns, including poleward shifts of biomes, primarily in response to temperature increases in high northern latitudes, as well as stability in desert and equatorial rainforest regions. This contrasts several previous studies that predicted widespread dieback of boreal and tropical forest dieback. The ranges of the proportion of grid cells affected by future biome shifts ranged between 4% and 56% for all models and RCPs considered in this study. Even in the low-emission scenario RCP2.6, biome changes were modeled and some regions are expected to experience low or even high susceptibility of biome change. Such change in the global distribution of biomes may imply substantial implications for ecosystem services and functions and thereby have strong impact on human societies (Parmesan et al., 2022). Our study can help identifying biomes and regions where biodiversity conservation, land management, and climate policy are most urgent.

Code availability. R scripts are provided in a Zenodo repository: https://tinyurl.com/2tjtpbk9

Data availability. (1) ISIMIP2b: GVM results for ISIMIP2b simulations downloaded from the ISIMIP repository: https://data.isimip.org
(2) Tuanmu and Jetz (2014): https://www.earthenv.org/landcover
(3) ESACCI, Harper et al. (2023): https://data.ceda.ac.uk/neodc/esacci/land_cover/data/pft/v2.0.8/
(4) 31 biome maps by Fischer et al. (2022): https://datadryad.org/stash/landing/show?id=doi%3A10.5061%2Fdryad.hqbzkh1jm

Author contributions. Simon Scheiter - Conceptualization, Data curation, Formal analysis, Investigation, Methodology, Project administration, Resources, Software, Validation, Visualization, Writing – original draft, Writing – review & editing; Jinfeng Chang - Data curation, Resources, Software; Philippe Ciais - Data curation, Resources, Software, Writing – review & editing; Marie Dury - Data curation, Resources, Software; Louis Francois - Data curation, Resources, Software, Writing – review& editing; Matthew Forrest - Data curation, Resources, Software, Writing – review & editing; Alexandra Henrot - Data curation, Resources, Software; Christopher P. O. Reyer - Data curation, Resources, Software, Writing – review & editing; Sonia Seneviratne - Data curation, Resources, Software; Jörg Steinkamp - Data curation, Resources, Software; Wim Thiery - Data curation, Resources, Software, Writing – review & editing; Wenfang Xu - Data curation, Resources, Software, Writing – review & editing; Thomas Hickler - Conceptualization, Data curation, Resources, Software, Writing – review & editing

Competing interests. The authors declare that they have no competing interests.

https://doi.org/10.5194/egusphere-2026-221
Preprint. Discussion started: 22 January 2026
© Author(s) 2026. CC BY 4.0 License.

Acknowledgements. MF, TH, JS gratefully acknowledge the computing time provided to them at the NHR Center NHR@SW at Goethe-University Frankfurt for the LPJ-GUESS simulations. This is funded by the Federal Ministry of Education and Research, and the state governments participating on the basis of the resolutions of the GWK for national high performance computing at universities (www.nhr-verein.de/unsere-partner). JC is supported by the National Key Research and Development Program (2022YFF0801904). WT acknowledges funding from the European Research Council (ERC) under the European Union's Horizon Framework research and innovation programme (grant agreement No 101124572; ERC Consolidator Grant 'LACRIMA'). The ISIMIP data team is acknowledged for maintaining the ISIMIP repository has enabled rapid and easy access to the data used in this study.

https://doi.org/10.5194/egusphere-2026-221
Preprint. Discussion started: 22 January 2026
© Author(s) 2026. CC BY 4.0 License.

References

Allen, J. R. M., Forrest, M., Hickler, T., Singarayer, J. S., Valdes, P. J., and Huntley, B.: Global vegetation patterns of the past 140,000 years, Journal of Biogeography, 47, 2073–2090, 2020.

Anderegg, W. R. L., Trugman, A. T., Badgley, G., Konings, A. G., and Shaw, J.: Divergent forest sensitivity to repeated extreme droughts, Nature Climate Change, 10, 1091–1095, https://doi.org/10.1038/s41558-020-00919-1, 2020.

Anders, T., Hetzer, J., Knapp, N., Forrest, M., Langan, L., Tölle, M. H., Wellbrock, N., and Hickler, T.: Modelling past and future impacts of droughts on tree mortality and carbon storage in Norway spruce stands in Germany, Ecological Modelling, 501, 110 987, https://doi.org/10.1016/j.ecolmodel.2024.110987, 2025.

Beierkuhnlein, C. and Fischer, J.-C.: Global biomes and ecozones – Conceptual and spatial communalities and discrepancies, Erdkunde, 75, 249–270, 2021.

Bertrand, R., Riofrio-Dillon, G., Lenoir, J., Drapier, J., de Ruffray, P., Gegout, J.-C., and Loreau, M.: Ecological constraints increase the climatic debt in forests, Nature Communications, 7, 12 643, 2016.

Blanco, C. C., Scheiter, S., Sosinski, E., Fidelis, A., Anand, M., and Pillar, V. D.: Feedbacks between vegetation and disturbance processes promote long-term persistence of forest–grassland mosaics in south Brazil, Ecological Modelling, 291, 224–232, https://doi.org/https://doi.org/10.1016/j.ecolmodel.2014.07.024, 2014.

Bonan, G. B.: Forests and climate change: Forcings, feedbacks, and the climate benefits of forests, Science, 320, 1444–1449, https://doi.org/10.1126/science.1155121, 2008.

Bonannella, C., Hengl, T., Parente, L., de Bruin, S., and Karabiniuk, M.: Biomes of the world under climate change scenarios: increasing aridity and higher temperatures lead to significant shifts in natural vegetation, PeerJ, 11, e15 593, https://doi.org/10.7717/peerj.15593, 2023.

Boonman, C. C. F., Huijbregts, M. A. J., Benítez-López, A., Schipper, A. M., Thuiller, W., and Santini, L.: Trait-based projections of climate change effects on global biome distributions, Diversity and Distributions, 28, 25–37, https://doi.org/https://doi.org/10.1111/ddi.13431, 2022.

Buchhorn, M., Smets, B., Bertels, L., De Roo, B., Lesiv, M., Tsendbazar, N.-E., Herold, M., and Fritz, S.: Copernicus Global Land Service: Land Cover 100m: collection 3: epoch 2015: Globe, https://doi.org/10.5281/zenodo.3939038, 2020.

Burton, C., Lampe, S., Kelley, D. I., Thiery, W., Hantson, S., Christidis, N., Gudmundsson, L., Forrest, M., Burke, E., Chang, J., Huang, H., Ito, A., Kou-Giesbrecht, S., Lasslop, G., Li, W., Nieradzik, L., Li, F., Chen, Y., Randerson, J., Reyer, C. P. O., and Mengel, M.: Global burned area increasingly explained by climate change, Nature Climate Change, 14, 1186–1192, https://doi.org/10.1038/s41558-024-02140-w, 2024.

Burton, C., Fang, L., Hantson, S., Forrest, M., Bradley, A., Burke, E., Chang, J., Chao, Y., Ciais, P., Huang, H., Ito, A., Kim, J., Kou-Giesbrecht, S., Nieradzik, L., Nishina, K., Ostberg, S., Zhu, Q., and Reyer, C. P.: ISIMIP3a Simulation Data from the Fire Sector, https://doi.org/10.48364/ISIMIP.446106.1, 2025.

Chambers, J. Q., Nogueira Lima, A. J., Pastorello, G., Gimenez, B. O., Meng, L., Dyer, L. A., Feng, Y., Santos da Silva, C., Costa de Oliveira, R., Weber, A., Koven, C., Negrón-Juárez, R., Spanner, G. C., Gaui, T. D., Fontes, C. G., de Araújo, A. C., McDowell, N., Leung, R., Marra, D. M., Warren, J., Celestina Souza, D., Wright, C., Jardine, K., Longo, M., Xu, C., Fine, P. V. A., Fisher, R. A., Tomasella, J., dos Santos, J., and Higuchi, N.: Hot droughts in the Amazon provide a window to a future hypertropical climate, Nature, https://doi.org/10.1038/s41586-025-09728-y, 2025.

https://doi.org/10.5194/egusphere-2026-221
Preprint. Discussion started: 22 January 2026
© Author(s) 2026. CC BY 4.0 License.

Champreux, A., Saltre, F., Traylor, W., Hickler, T., and Bradshaw, C. J. A.: How to map biomes: Quantitative comparison and review of biome-mapping methods, Ecological Monographs, 94, e1615, https://doi.org/10.1002/ecm.1615, 2024.

Choury, Z., Wujeska-Klause, A., Bourne, A., Bown, N. P., Tjoelker, M. G., Medlyn, B. E., and Crous, K. Y.: Tropical rainforest species have larger increases in temperature optima with warming than warm-temperate rainforest trees, New Phytol, 234, 1220–1236, https://doi.org/10.1111/nph.18077, 2022.

Conradi, T., Eggli, U., Kreft, H., Schweiger, A. H., Weigelt, P., and Higgins, S. I.: Reassessment of the risks of climate change for terrestrial ecosystems, Nature Ecology & Evolution, 8, 888–900, https://doi.org/10.1038/s41559-024-02333-8, 2024.

Dallmeyer, A., Claussen, M., and Brovkin, V.: Harmonising plant functional type distributions for evaluating Earth system models, Climate of the Past, 15, 335–366, https://doi.org/10.5194/cp-15-335-2019, 2019.

Doughty, C. E., Keany, J. M., Wiebe, B. C., Rey-Sanchez, C., Carter, K. R., Middleby, K. B., Cheesman, A. W., Goulden, M. L., da Rocha, H. R., Miller, S. D., Malhi, Y., Fauset, S., Gloor, E., Slot, M., Oliveras Menor, I., Crous, K. Y., Goldsmith, G. R., and Fisher, J. B.: Tropical forests are approaching critical temperature thresholds, Nature, 621, 105–111, https://doi.org/10.1038/s41586-023-06391-z, 2023.

Fernandez-Delgado, M., Cernadas, E., Barro, S., and Amorim, D.: Do we Need Hundreds of Classifiers to Solve Real World Classification Problems?, Journal of Machine Learning Research, 15, 3133–3181, 2014.

Fischer, J.-C., Walentowitz, A., and Beierkuhnlein, C.: The biome inventory - standardizing global biogeographical land units, Global Ecology and Biogeography, 31, 2172–2183, https://doi.org/https://doi.org/10.1111/geb.13574, 2022.

Fischer, R., Anders, T., Bugmann, H., Djahangard, M., Dreßler, G., Hetzer, J., Hickler, T., Hiltner, U., Marano, G., Sperlich, D., Yousefpour, R., and Knapp, N.: Perspectives for forest modeling to improve the representation of drought-related tree mortality, https://doi.org/10.5073/JfK.2025.02.05, 2025.

Frieler, K., Lange, S., Piontek, F., Reyer, C. P. O., Schewe, J., Warszawski, L., Zhao, F., Chini, L., Denvil, S., Emanuel, K., Geiger, T., Halladay, K., Hurtt, G., Mengel, M., Murakami, D., Ostberg, S., Popp, A., Riva, R., Stevanovic, M., Suzuki, T., Volkholz, J., Burke, E., Ciais, P., Ebi, K., Eddy, T. D., Elliott, J., Galbraith, E., Gosling, S. N., Hattermann, F., Hickler, T., Hinkel, J., Hof, C., Huber, V., Jägermeyr, J., Krysanova, V., Marcé, R., Müller Schmied, H., Mouratiadou, I., Pierson, D., Tittensor, D. P., Vautard, R., van Vliet, M., Biber, M. F., Betts, R. A., Bodirsky, B. L., Deryng, D., Frolking, S., Jones, C. D., Lotze, H. K., Lotze-Campen, H., Sahajpal, R., Thonicke, K., Tian, H., and Yamagata, Y.: Assessing the impacts of 1.5°C global warming - simulation protocol of the Inter-Sectoral Impact Model Intercomparison Project (ISIMIP2b), Geoscientific Model Development, 10, 4321–4345, https://doi.org/10.5194/gmd-10-4321-2017, 2017.

Gonzalez, P., Neilson, R. P., Lenihan, J. M., and Drapek, R. J.: Global patterns in the vulnerability of ecosystems to vegetation shifts due to climate change, Global Ecology and Biogeography, 19, 755–768, https://doi.org/https://doi.org/10.1111/j.1466-8238.2010.00558.x, 2010.

Guimberteau, M., Zhu, D., Maignan, F., Huang, Y., Yue, C., Dantec-Nédélec, S., Ottlé, C., Jornet-Puig, A., Bastos, A., Laurent, P., Goll, D., Bowring, S., Chang, J., Guenet, B., Tifafi, M., Peng, S., Krinner, G., Ducharne, A., Wang, F., Wang, T., Wang, X., Wang, Y., Yin, Z., Lauerwald, R., Joetzjer, E., Qiu, C., Kim, H., and Ciais, P.: ORCHIDEE-MICT (v8.4.1), a land surface model for the high latitudes: model description and validation, Geoscientific Model Development, 11, 121–163, https://doi.org/10.5194/gmd-11-121-2018, 2018.

Hantson, S., Arneth, A., Harrison, S. P., Kelley, D. I., Prentice, I. C., Rabin, S. S., Archibald, S., Mouillot, F., Arnold, S. R., Artaxo, P., Bachelet, D., Ciais, P., Forrest, M., Friedlingstein, P., Hickler, T., Kaplan, J. O., Kloster, S., Knorr, W., Lasslop, G., Li, F., Mangeon, S., Melton, J. R., Meyn, A., Sitch, S., Spessa, A., van der Werf, G. R., Voulgarakis, A., and Yue, C.: The status and challenge of global fire modelling, Biogeosciences, 13, 3359–3375, https://doi.org/10.5194/bg-13-3359-2016, 2016.

https://doi.org/10.5194/egusphere-2026-221
Preprint. Discussion started: 22 January 2026
© Author(s) 2026. CC BY 4.0 License.

Harper, K. L., Lamarche, C., Hartley, A., Peylin, P., Ottlé, C., Bastrikov, V., San Martín, R., Bohnenstengel, S. I., Kirches, G., Boettcher, M., Shevchuk, R., Brockmann, C., and Defourny, P.: A 29-year time series of annual 300 m resolution plant-functional-type maps for climate models, Earth System Science Data, 15, 1465–1499, https://doi.org/10.5194/essd-15-1465-2023, 2023.

Hetzer, J., Forrest, M., Ribalaygua, J., Prado-López, C., and Hickler, T.: The fire weather in Europe: large-scale trends towards higher danger, Environmental Research Letters, 19, 084 017, https://doi.org/10.1088/1748-9326/ad5b09, 2024.

Hickler, T., Prentice, I. C., Smith, B., Sykes, M. T., and Zaehle, S.: Implementing plant hydraulic architecture within the LPJ Dynamic Global Vegetation Model, Global Ecology and Biogeography, 15, 567–577, 2006.

Hickler, T., Vohland, K., Feehan, J., Miller, P. A., Smith, B., Costa, L., Giesecke, T., Fronzek, S., Carter, T. R., Cramer, W., Kuhn, I., and Sykes, M. T.: Projecting the future distribution of European potential natural vegetation zones with a generalized, tree species-based dynamic vegetation model, Global Ecology and Biogeography, 21, 50–63, https://doi.org/10.1111/j.1466-8238.2010.00613.x, 2012.

Higgins, S. I. and Scheiter, S.: Atmospheric CO_2 forces abrupt vegetation shifts locally, but not globally., Nature, 488, 209–212, 2012.

Hijmans, R. J.: terra: Spatial Data Analysis. R package version 1.7-71, https://CRAN.R-project.org/package=terra, 2024.

Huntley, B., Collingham, Y. C., Singarayer, J. S., Valdes, P. J., Barnard, P., Midgley, G. F., Altwegg, R., and Ohlem"uller, R.: Explaining patterns of avian diversity and endemicity: climate and biomes of southern Africa over the last 140,000 years, Journal of Biogeography, 43, 874–886, https://doi.org/10.1111/jbi.12714, 2016.

Klein Goldewijk, K., Beusen, A., Doelman, J., and Stehfest, E.: Anthropogenic land use estimates for the Holocene – HYDE 3.2, Earth System Science Data, 9, 927–953, https://doi.org/10.5194/essd-9-927-2017, 2017.

Kumar, D., Pfeiffer, M., Gaillard, C., Langan, L., Martens, C., and Scheiter, S.: Misinterpretation of Asian savannas as degraded forest can mislead management and conservation policy under climate change, Biological Conservation, 241, 108 293, 2020.

Langan, L., Scheiter, S., Hickler, T., and Higgins, S. I.: Amazon forest resistance to drought isincreased by diversity in hydraulic traits, Nature Communications, 16, 8246, 2025.

Lange, S.: Bias correction of surface downwelling longwave and shortwave radiation for the EWEMBI dataset, Earth System Dynamics, 9, 627–645, https://doi.org/10.5194/esd-9-627-2018, 2018.

Lange, S.: EartH2Observe, WFDEI and ERA-Interim data Merged and Bias-corrected for ISIMIP (EWEMBI). V. 1.1., GFZ Data Services, https://doi.org/https://doi.org/10.5880/pik.2019.004, 2019.

Lasslop, G., Hantson, S., Harrison, S. P., Bachelet, D., Burton, C., Forkel, M., Forrest, M., Li, F., Melton, J. R., Yue, C., Archibald, S., Scheiter, S., Arneth, A., Hickler, T., and Sitch, S.: Global ecosystems and fire: Multi-model assessment of fire-induced tree-cover and carbon storage reduction, Global Change Biology, 26, 5027–5041, https://doi.org/10.1111/gcb.15160, 2020.

Lenormand, T., Roze, D., and Rousset, F.: Stochasticity in evolution, Trends in Ecology & Evolution, 24, 157–165, 2009.

Liaw, A. and Wiener, M.: Classification and Regression by randomForest, R News, 2, 18–22, https://CRAN.R-project.org/doc/Rnews/, 2002.

Loarie, S. R., Duffy, P. B., Hamilton, H., Asner, G. P., Field, C. B., and Ackerly, D. D.: The velocity of climate change, Nature, 462, 1052—1055, https://doi.org/10.1038/nature08649, 2009.

Lucht, W., Prentice, I. C., Myneni, R. B., Sitch, S., Friedlingstein, P., Cramer, W., Bousquet, P., Buermann, W., and Smith, B.: Climatic Control of the High-Latitude Vegetation Greening Trend and Pinatubo Effect, Science, 296, 1687–1689, https://doi.org/10.1126/science.1071828, 2002.

MacCarthy, J., Tyukavina, A., Weisse, M. J., Harris, N., and Glen, E.: Extreme wildfires in Canada and their contribution to global loss in tree cover and carbon emissions in 2023, Global Change Biology, 30, e17 392, https://doi.org/10.1111/gcb.17392, 2024.

https://doi.org/10.5194/egusphere-2026-221
Preprint. Discussion started: 22 January 2026
© Author(s) 2026. CC BY 4.0 License.

Martens, C., Hickler, T., Davis-Reddy, C., Engelbrecht, F., Higgins, S. I., von Maltitz, G. P., Midgley, G. F., Pfeiffer, M., and Scheiter, S.: Large uncertainties in future biome changes in Africa call for flexible climate adaptation strategies, Global Change Biology, 27, 340–358, https://doi.org/10.1111/gcb.15390, 2021.

McDowell, N., Allen, C. D., Anderson-Teixeira, K., Brando, P., Brienen, R., Chambers, J., Christoffersen, B., Davies, S., Doughty, C., Duque, A., Espirito-Santo, F., Fisher, R., Fontes, C. G., Galbraith, D., Goodsman, D., Grossiord, C., Hartmann, H., Holm, J., Johnson, D. J., Kassim, A. R., Keller, M., Koven, C., Kueppers, L., Kumagai, T., Malhi, Y., McMahon, S. M., Mencuccini, M., Meir, P., Moorcroft, P., Muller-Landau, H. C., Phillips, O. L., Powell, T., Sierra, C. A., Sperry, J., Warren, J., Xu, C., and Xu, X.: Drivers and mechanisms of tree mortality in moist tropical forests, New Phytologist, 219, 851–869, https://doi.org/10.1111/nph.15027, 2018.

Midgley, G. F. and Bond, W. J.: Future of African terrestrial biodiversity and ecosystems under anthropogenic climate change, Nature Clim. Change, 5, 823–829, http://dx.doi.org/10.1038/nclimate2753, 2015.

Minet, J., Laloy, E., Tychon, B., and François, L.: Bayesian inversions of a dynamic vegetation model at four European grassland sites, Biogeosciences, 12, 2809–2829, https://doi.org/10.5194/bg-12-2809-2015, 2015.

Monserud, R. A. and Leemans, R.: Comparing global vegetation maps with the kappa-statistic, Ecological Modelling, 62, 275–293, 1992.

Mucina, L.: Biome: evolution of a crucial ecological and biogeographical concept, New Phytologist, 222, 97–114, https://doi.org/10.1111/nph.15609, 2019.

Newbold, T., Hudson, L. N., Arnell, A. P., Contu, S., De Palma, A., Ferrier, S., Hill, S. L. L., Hoskins, A. J., Lysenko, I., Phillips, H. R. P., Burton, V. J., Chng, C. W. T., Emerson, S., Gao, D., Pask-Hale, G., Hutton, J., Jung, M., Sanchez-Ortiz, K., Simmons, B. I., Whitmee, S., Zhang, H., Scharlemann, J. P. W., and Purvis, A.: Has land use pushed terrestrial biodiversity beyond the planetary boundary? A global assessment, Science, 353, 288–291, https://doi.org/10.1126/science.aaf2201, 2016.

Olson, D. M., Dinerstein, E., Wikramanayake, E. D., Burgess, N. D., Powell, G. V. N., Underwood, E. C., D'amico, J. A., Itoua, I., Strand, H. E., Morrison, J. C., Loucks, C. J., Allnutt, T. F., Ricketts, T. H., Kura, Y., Lamoreux, J. F., Wettengel, W. W., Hedao, P., and Kassem, K. R.: Terrestrial Ecoregions of the World: A New Map of Life on Earth: A new global map of terrestrial ecoregions provides an innovative tool for conserving biodiversity, BioScience, 51, 933–938, https://doi.org/10.1641/0006-3568(2001)051[0933:TEOTWA]2.0.CO;2, 2001.

Parmesan, C., Morecroft, M. D., Trisurat, Y., Adrian, R., Anshari, G. Z., Arneth, A., Gao, Q., Gonzalez, P., Harris, R., Price, J., Stevens, N., and Talukdarr, G. H.: Climate Change 2022: Impacts, Adaptation and Vulnerability. Contribution of Working Group II to the Sixth Assessment Report of the Intergovernmental Panel on Climate Change, chap. Terrestrial and Freshwater Ecosystems and Their Services, pp. 197–377, Cambridge University Press, Cambridge, UK and New York, NY, USA, https://doi.org/10.1017/9781009325844.004, 2022.

Parry, I. M., Ritchie, P. D. L., and Cox, P. M.: Evidence of localised Amazon rainforest dieback in CMIP6 models, Earth System Dynamics, 13, 1667–1675, https://doi.org/10.5194/esd-13-1667-2022, 2022.

Pausas, J. G. and Bond, W. J.: Alternative Biome States in Terrestrial Ecosystems, Trends in Plant Science, 25, 250–263, https://doi.org/10.1016/j.tplants.2019.11.003, 2020.

Popp, A., Humpenöder, F., Weindl, I., Bodirsky, B. L., Bonsch, M., Lotze-Campen, H., Müller, C., Biewald, A., Rolinski, S., Stevanovic, M., and Dietrich, J. P.: Land-use protection for climate change mitigation, Nature Climate Change, 4, 1095–1098, https://doi.org/10.1038/nclimate2444, 2014.

Prentice, I. C., Cramer, W., Harrison, S. P., Leemans, R., Monserud, R. A., and Solomon, A. M.: A global biome model based on plant physiology and dominance, soil properties and climate, Journal of Biogeography, 19, 117–134, 1992.

https://doi.org/10.5194/egusphere-2026-221
Preprint. Discussion started: 22 January 2026
© Author(s) 2026. CC BY 4.0 License.

Prentice, I. C., Bondeau, A., Cramer, W., Harrison, S. P., Hickler, T., Lucht, W., Sitch, S., Smith, B., and Sykes, M. T.: Terrestrial Ecosystems in a Changing World, chap. Dynamic Global Vegetation Modeling: Quantifying Terrestrial Ecosystem Responses to Large-Scale Environmental Change, pp. 175–192, Springer, 2007.

R Core Team: R: A Language and Environment for Statistical Computing, R Foundation for Statistical Computing, Vienna, Austria, https://www.R-project.org/, 2024.

Rammig, A., Jupp, T., Thonicke, K., Tietjen, B., Heinke, J., Ostberg, S., Lucht, W., Cramer, W., and Cox, P.: Estimating the risk of Amazonian forest dieback, New Phytologist, 187, 694–706, https://doi.org/10.1111/j.1469-8137.2010.03318.x, 2010.

Reyer, C. P., Chang, J., Arneth, A., Chen, M., Forrest, M., François, L., Henrot, A., Hickler, T., Ito, A., Kim, J., Kutschera, E., Mathison, C., Nishina, K., Ostberg, S., Pan, S., Ren, W., Schaphoff, S., Seneviratne, S., Steinkamp, J., Thiery, W., Tian, H., Xu, W., Yang, J., Zhao, F., Büchner, M., and Ciais, P.: ISIMIP2b Simulation Data from the Global Biomes Sector, https://doi.org/10.48364/ISIMIP.223634.2, 2024.

Sanderson, E. W., Jaiteh, M., Levy, M. A., Redford, K. H., Wannebo, A. V., and Woolmer, G.: The Human Footprint and the Last of the Wild: The human footprint is a global map of human influence on the land surface, which suggests that human beings are stewards of nature, whether we like it or not, BioScience, 52, 891–904, https://doi.org/10.1641/0006-3568(2002)052[0891:THFATL]2.0.CO;2, 2002.

Scheiter, S. and Savadogo, P.: Ecosystem management can mitigate vegetation shifts induced by climate change in West Africa, Ecological Modelling, 332, 19–27, https://doi.org/10.1016/j.ecolmodel.2016.03.022, 2016.

Scheiter, S., Langan, L., and Higgins, S. I.: Next generation dynamic global vegetation models: learning from community ecology, New Phytologist, 198, 957–969, https://doi.org/10.1111/nph.12210, 2013.

Scheiter, S., Gaillard, C., Martens, C., Erasmus, B., and Pfeiffer, M.: How vulnerable are ecosystems in the Limpopo province to climate change?, South African Journal of Botany, 116, 86 – 95, https://doi.org/https://doi.org/10.1016/j.sajb.2018.02.394, 2018.

Scheiter, S., Moncrieff, G. R., Pfeiffer, M., and Higgins, S. I.: African biomes are most sensitive to changes in CO_2 under recent and near-future CO_2 conditions, Biogeosciences, 17, 1147—1167, 2020.

Scheiter, S., Kumar, D., Pfeiffer, M., and Langan, L.: Biome classification influences current and projected future biome distributions, Global Ecology and Biogeography, 33, 259–271, 2024a.

Scheiter, S., Kumar, D., Pfeiffer, M., and Langan, L.: Modeling drought mortality and resilience of savannas and forests in tropical Asia, Ecological Modelling, 494, 110 783, https://doi.org/10.1016/j.ecolmodel.2024.110783, 2024b.

Schleuning, M., Fründ, J., Schweiger, O., Welk, E., Albrecht, J., Albrecht, M., Beil, M., Benadi, G., Blüthgen, N., Bruelheide, H., Böhning-Gaese, K., Dehling, D. M., Dormann, C. F., Exeler, N., Farwig, N., Harpke, A., Hickler, T., Kratochwil, A., Kuhlmann, M., Kühn, I., Michez, D., Mudri-Stojnić, S., Plein, M., Rasmont, P., Schwabe, A., Settele, J., Vujić, A., Weiner, C. N., Wiemers, M., and Hof, C.: Ecological networks are more sensitive to plant than to animal extinction under climate change, Nature Communications, 7, 13 965, https://doi.org/10.1038/ncomms13965, 2016.

Schultz, J.: "Okozonen der Erde, Eugen Ulmer UTB, 5. edn., 2016.

Shi, H., Tian, H., Lange, S., Yang, J., Pan, S., Fu, B., and Reyer, C. P. O.: Terrestrial biodiversity threatened by increasing global aridity velocity under high-level warming, Proceedings of the National Academy of Sciences, 118, e2015552 118, https://doi.org/10.1073/pnas.2015552118, 2021.

Sitch, S., Smith, B., Prentice, I. C., Arneth, A., Bondeau, A., Cramer, W., Kaplan, J. O., Levis, S., Lucht, W., Sykes, M. T., Thonicke, K., and Venevsky, S.: Evaluation of ecosystem dynamics, plant geography and terrestrial carbon cycling in the LPJ dynamic global vegetation model, Global Change Biology, 9, 161–185, 2003.

https://doi.org/10.5194/egusphere-2026-221
Preprint. Discussion started: 22 January 2026
© Author(s) 2026. CC BY 4.0 License.

Sitch, S., Huntingford, C., Gedney, N., Levy, P. E., Lomas, M., Piao, S. L., Betts, R., Ciais, P., Cox, P., Friedlingstein, P., Jones, C. D., Prentice, I. C., and Woodward, F. I.: Evaluation of the terrestrial carbon cycle, future plant geography and climate-carbon cycle feedbacks using five Dynamic Global Vegetation Models (DGVMs), Global Change Biology, 14, 2015–2039, 2008.

Sjoberg, D.: ggsankey: Sankey, Alluvial and Sankey Bump Plots, https://github.com/davidsjoberg/ggsankey, r package version 0.0.99999, commit b675d0d5144b1b5758d3b2b41e86ceee66a1e071, 2024.

Smith, B., Wårlind, D., Arneth, A., Hickler, T., Leadley, P., Siltberg, J., and Zaehle, S.: Implications of incorporating N cycling and N limitations on primary production in an individual-based dynamic vegetation model, Biogeosciences, 11, 2027–2054, https://doi.org/10.5194/bg-11-2027-2014, 2014.

Snell, R. S., Huth, A., Nabel, J. E. M. S., Bocedi, G., Travis, J. M. J., Gravel, D., Bugmann, H., Gutierrez, A. G., Hickler, T., Higgins, S. I., Reineking, B., Scherstjanoi, M., Zurbriggen, N., and Lischke, H.: Using dynamic vegetation models to simulate plant range shifts, Ecography, 37, 1184–1197, https://doi.org/10.1111/ecog.00580, 2014.

Stevanović, M., Popp, A., Lotze-Campen, H., Dietrich, J. P., Müller, C., Bonsch, M., Schmitz, C., Bodirsky, B. L., Humpenöder, F., and Weindl, I.: The impact of high-end climate change on agricultural welfare, Science Advances, 2, e1501 452, https://doi.org/10.1126/sciadv.1501452, 2016.

Tateishi, R., Bayaer, U., Al-Bilbisi, H., Aboel Ghar, M., Tsend-Ayush, J., Kobayashi, T., Kasimu, A., Hoan, N. T., Shalaby, A., Alsaaideh, B., Enkhzaya, T., G., and Sato, H. P.: Production of global land cover data - GLCNMO, International Journal of Digital Earth, 4, 22–49, https://doi.org/10.1080/17538941003777521, 2011.

Tateishi, R., Thanh Hoan, N., Kobayashi, T., Alsaaideh, B., Tana, G., and Xuan Phong, D.: Production of global land cover data - GLCNMO2008, Journal of Geography and Geology, 6, 99–122, 2014.

The Nature Conservancy: Global ecoregions, major habitat types, biogeographical realms and the nature conservancy terrestrial assessment units as of December 14, 2009, Tech. rep., The Nature Conservancy, 2009.

Thiery, W., Davin, E. L., Lawrence, D. M., Hirsch, A. L., Hauser, M., and Seneviratne, S. I.: Present-day irrigation mitigates heat extremes, Journal of Geophysical Research: Atmospheres, 122, 1403–1422, https://doi.org/10.1002/2016JD025740, 2017.

Tobian, A., Gerten, D., Fetzer, I., Schaphoff, S., Andersen, L. S., Cornell, S., and Rockström, J.: Climate change critically affects the status of the land-system change planetary boundary, Environmental Research Letters, 19, 054 060, https://doi.org/10.1088/1748-9326/ad40c2, 2024.

Tuanmu, M.-N. and Jetz, W.: A global 1-km consensus land-cover product for biodiversity and ecosystem modelling, Global Ecology and Biogeography, 23, 1031–1045, https://doi.org/10.1111/geb.12182, 2014.

Walter, H.: Die Vegetation der Erde in "oko-physiologischer Betrachtung. Band 1: Die tropischen und subtropischen Zonen, VEB Gustav Fischer, 1964.

Wang, L., Arora, V. K., Bartlett, P., Chan, E., and Curasi, S. R.: Mapping of ESA's Climate Change Initiative land cover data to plant functional types for use in the CLASSIC land model, Biogeosciences, 20, 2265–2282, https://doi.org/10.5194/bg-20-2265-2023, 2023.

Warnant, P., Francois, L., Strivay, D., and Gerard, J.-C.: CARAIB: A global model of terrestrial biological productivity, Global Biogeochemical Cycles, 8, 255–270, https://doi.org/https://doi.org/10.1029/94GB00850, 1994.

Wickham, H.: ggplot2: Elegant Graphics for Data Analysis, Springer-Verlag New York, https://ggplot2.tidyverse.org, 2016.

Zani, D., Lehsten, V., and Lischke, H.: Tree migration in the dynamic, global vegetation model LPJ-GM 1.1: efficient uncertainty assessment and improved dispersal kernels of European trees, Geoscientific Model Development, 15, 4913–4940, https://doi.org/10.5194/gmd-15-4913-2022, 2022.

https://doi.org/10.5194/egusphere-2026-221
Preprint. Discussion started: 22 January 2026
© Author(s) 2026. CC BY 4.0 License.

Zani, D., Lischke, H., and Lehsten, V.: The role of dispersal limitation in the forest biome shifts of Europe in the last 18,000 yeary, Journal of Biogeography, 51, 1438–1457, https://doi.org/10.1111/jbi.14836, 2024.

https://doi.org/10.5194/egusphere-2026-221
Preprint. Discussion started: 22 January 2026
© Author(s) 2026. CC BY 4.0 License.

Table 1. Performance of random forest models for temperature-limited biomes versus other biomes. The κ was averaged for all biomes in the Olson et al. (2001) biome map that are considered to be mainly limited by temperature or not (i.e., by other factors, see Table S2). Differences between those values were calculated and p-values of t-tests are provided. For the GVMs, only results for RCP6.0 are provided; the results for RCP2.6 and RCP8.5 under current climate are similar (not shown).

Data	κ temp driven	κ other factors	Difference	p-value
LPJ-GUESS	0.683	0.359	0.324	0.048
ORCHIDEE	0.857	0.730	0.127	0.153
ORCHIDEE-DGVM	0.894	0.691	0.203	0.080
CARAIB	0.947	0.980	-0.033	0.121
CLM	0.735	0.406	0.329	0.015
ESACCI	0.957	0.894	0.063	0.101
Tuanmu	0.993	0.987	0.006	0.351

https://doi.org/10.5194/egusphere-2026-221
Preprint. Discussion started: 22 January 2026
© Author(s) 2026. CC BY 4.0 License.

Table 2. Biome change for temperature-limited biomes versus other biomes. The proportion of grid cells affected by biome change between current and future conditions was averaged for all biomes in the Olson et al. (2001) biome map that are considered to be mainly limited by temperature or not (i.e., by other factors, see Table S2). Differences between those values were calculated and p-values of t-tests are provided.

RCP	Data	Δ temp driven	Δ other factors	Difference	p-value
RCP2.6	LPJ-GUESS	33.93	54.78	-20.85	0.26
RCP2.6	ORCHIDEE	12.97	36.60	-23.63	0.05
RCP2.6	ORCHIDEE-DGVM	32.02	54.66	-22.64	0.20
RCP2.6	CARAIB	29.18	49.99	-20.81	0.21
RCP2.6	CLM	6.40	21.23	-14.83	0.13
RCP6.0	LPJ-GUESS	42.49	57.25	-14.76	0.44
RCP6.0	ORCHIDEE	20.35	39.72	-19.37	0.15
RCP6.0	ORCHIDEE-DGVM	39.11	61.65	-22.54	0.22
RCP6.0	CARAIB	42.87	59.14	-16.27	0.36
RCP6.0	CLM	9.13	32.83	-23.70	0.13
RCP8.5	LPJ-GUESS	52.69	68.71	-16.02	0.42
RCP8.5	ORCHIDEE	24.16	49.18	-25.02	0.12
RCP8.5	CLM	20.19	54.40	-34.21	0.10

https://doi.org/10.5194/egusphere-2026-221
Preprint. Discussion started: 22 January 2026
© Author(s) 2026. CC BY 4.0 License.

Figure 1. Data-model agreement for different biome maps. For each F31 biome map and each biome map derived from classifying PFTs into biomes, the κ value was calculated. Here, all biomes globally were considered, i.e., κ values were not calculated per biome. Biome classification was conducted with PFT-specific LAI for GVMs and PFT cover for remote sensing products. For the GVMs, simulations for RCP6.0 were used (other RCPs not shown).

https://doi.org/10.5194/egusphere-2026-221
Preprint. Discussion started: 22 January 2026
© Author(s) 2026. CC BY 4.0 License.

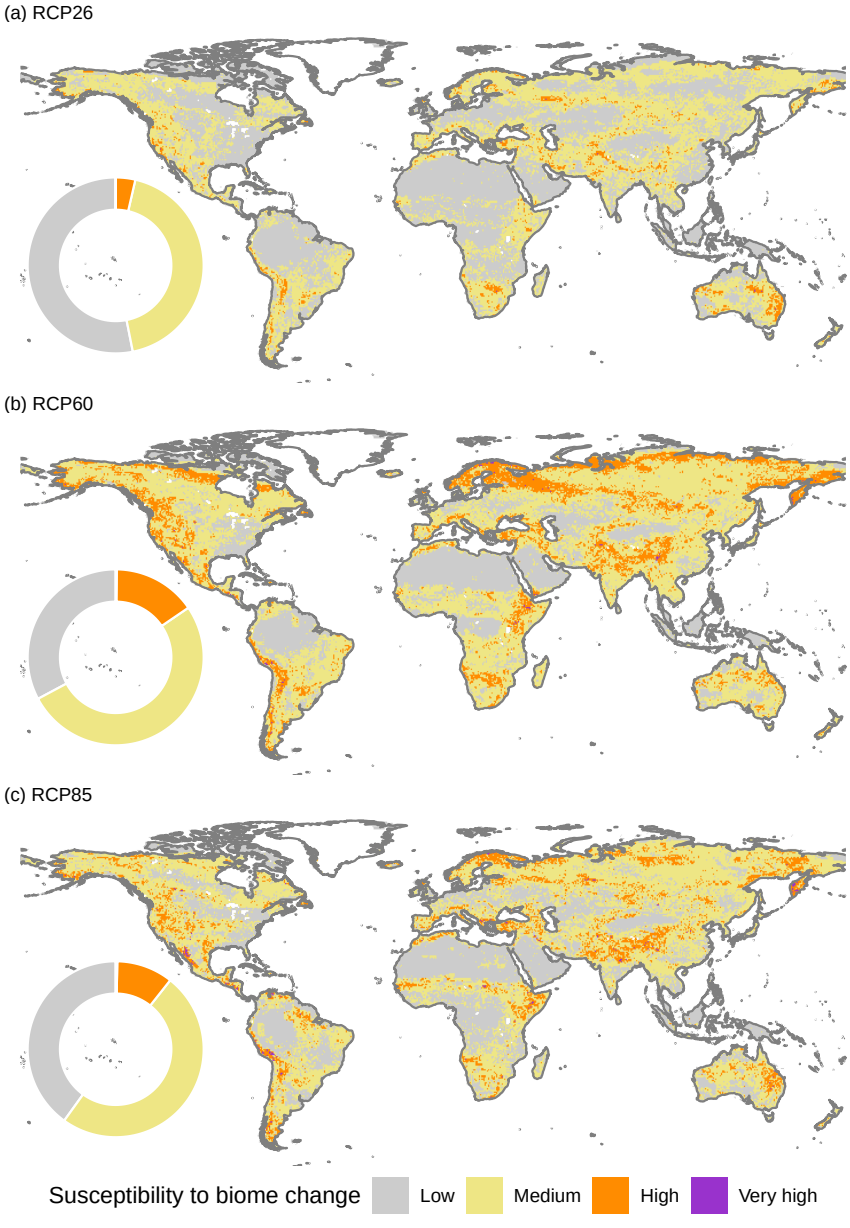

Figure 2. Susceptibility to biome change for different RCP scenarios for all GVMs and all 31 biome maps. The maps show the susceptibility categories derived from the number of models that project a biome change until the end of the century for all combinations of the F31 biome maps and all GVMs available for different RCPs. The circle plots indicate the proportion of the land surface in different categories. Susceptibility categories are Low: 0 to 20% of the models predict biome shift; Medium: 20 to 40%; High: 40 to 60%; Very high: more than 60%. Note that for RCP2.6 and RCP6.0, 5 different GVMs were available, but only 3 GVMs for RCP8.5. Hence, the categories refer to 155 and 93 biome maps derived from random forest classification.

https://doi.org/10.5194/egusphere-2026-221
Preprint. Discussion started: 22 January 2026
© Author(s) 2026. CC BY 4.0 License.

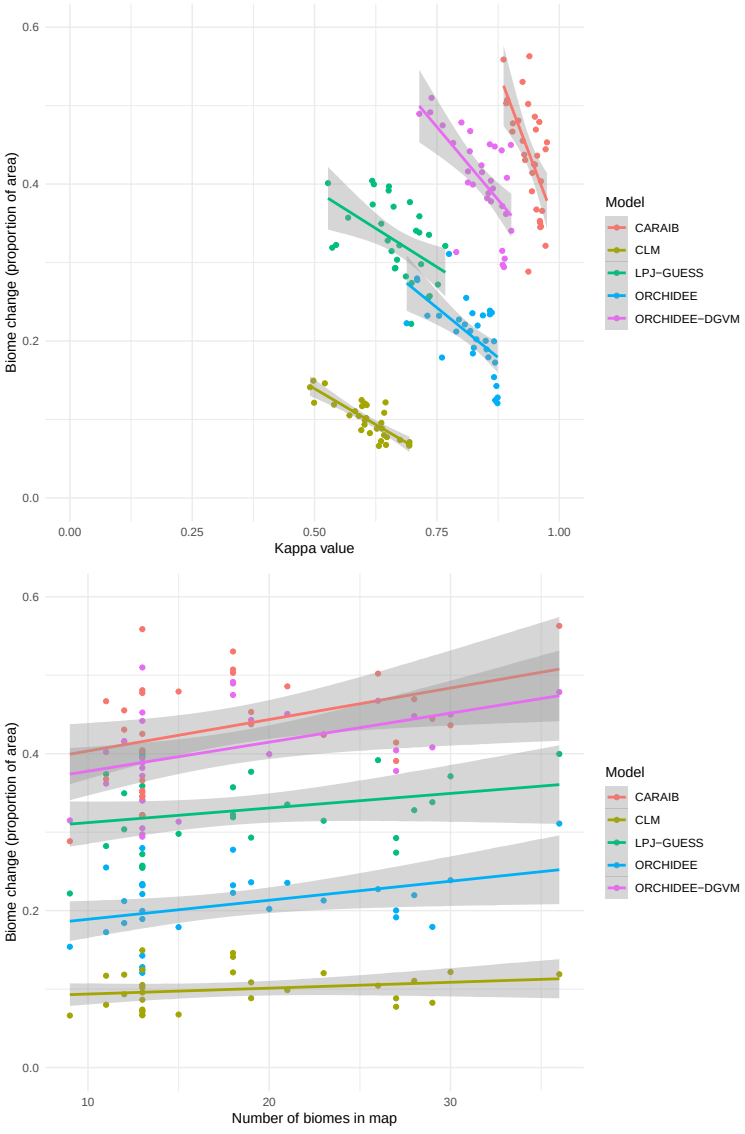

Figure 3. Rate of biome change in relation to data-model agreement and the number of biomes. Each point represents a biome classification for one of the F31 biome maps. The κ values were calculated for all biomes in the respective data-model combination. Change represents the proportion of grid cells undergoing biome transitions until the end of the century for a given GVM and biome classification. Figures represent RCP6.0, results for all RCPs are provided in the supplement.

https://doi.org/10.5194/egusphere-2026-221
Preprint. Discussion started: 22 January 2026
© Author(s) 2026. CC BY 4.0 License.

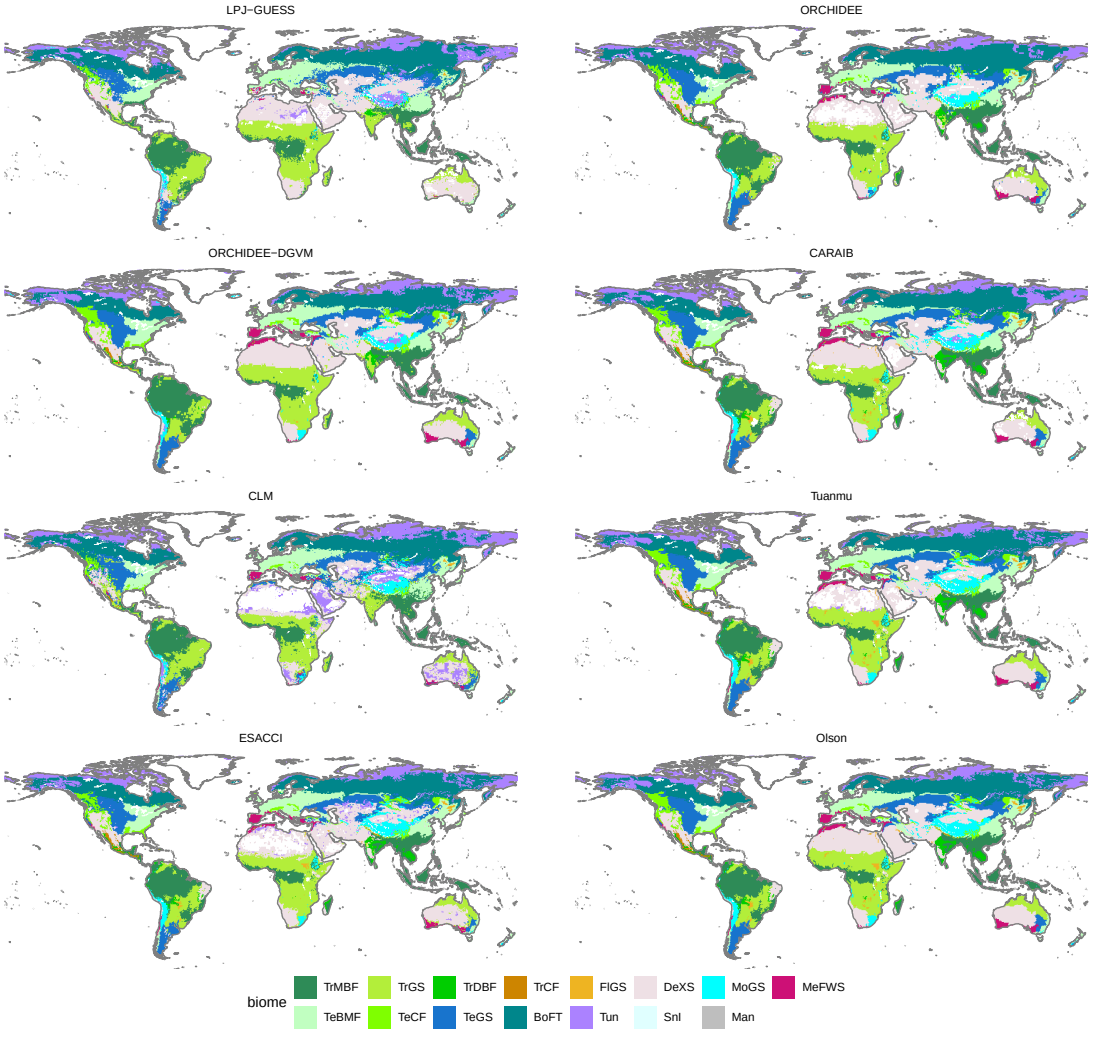

Figure 4. Modeled and observation-based biome maps. The maps show the modeled biome distributions for different GVMs and PFT products classified for the Olson et al. (2001) biome map for RCP6.0. Biomes: TrMBF -Tropical and subtropical moist broadleaf forest; TrGS - Tropical and subtropical grassland savanna and shrubland; TrDBF - Tropical and subtropical dry broadleaf forest; TrCF - Tropical and subtropical coniferous forest; FlGS - Flooded grassland and savanna; DeXS - Deserts and xeric shrubland; MoGS - Montane grassland and shrubland; MeFWS - Mediterranean forest woodland and scrub; TeBMF - Temperate broadleaf and mixed forest; TeCF - Temperate conifer forest; TeGS - Temperate grassland savanna and shrubland; BoFT - Boreal forest/taiga; Tun - Tundra.

https://doi.org/10.5194/egusphere-2026-221
Preprint. Discussion started: 22 January 2026
© Author(s) 2026. CC BY 4.0 License.

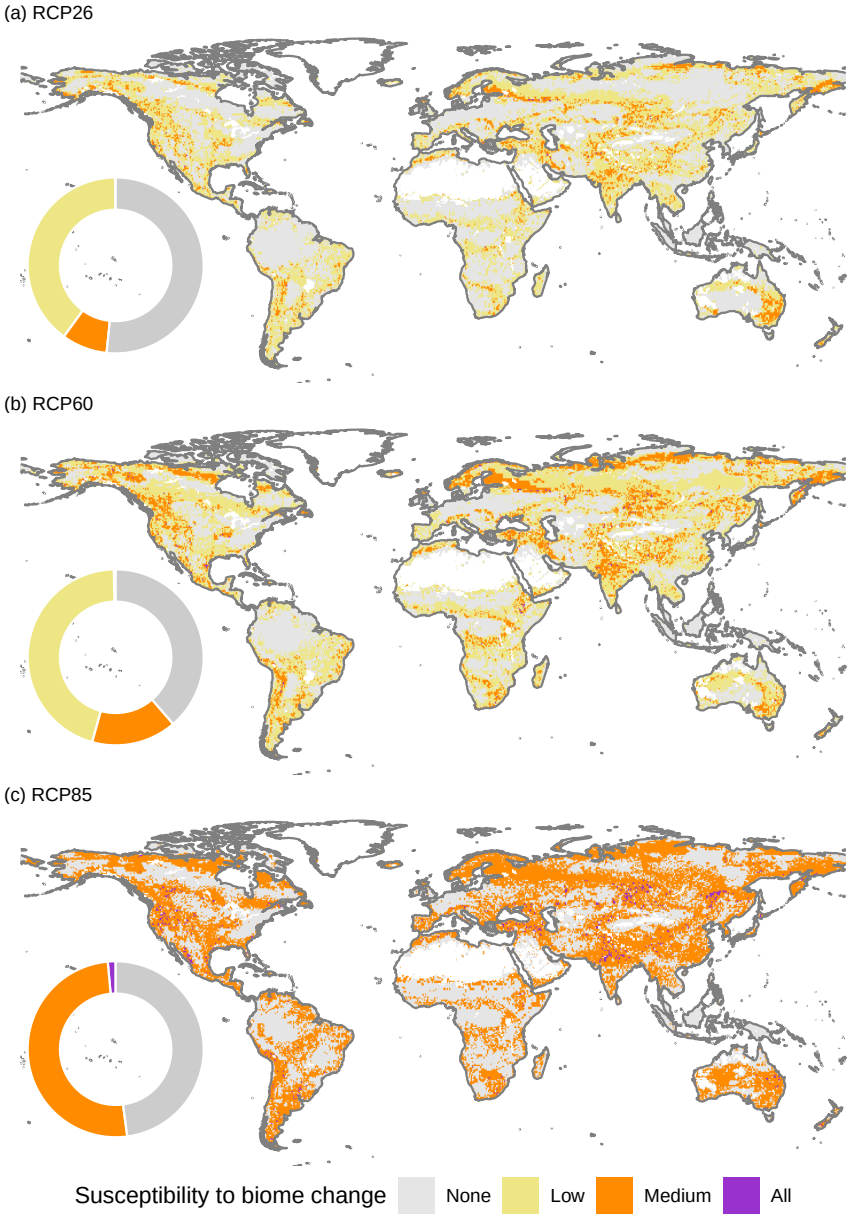

Figure 5. Hotspots of biome shifts for Olson et al. (2001) map. The maps show the number of GVMs projecting a biome shift until the end of the century under different RCPs when biomes were classified using the Olson et al. (2001) biome map. For RCP2.6 and RCP6.0, 5 GVMs were available, and 'Low' and 'Medium' indicate agreement of 1 or 2 and 3 or 4 models, respectively. For RCP8.5, 3 different GVMs were available, and 'Medium' indicates that 1 or 2 models agree. Category 'Low' is not used.

https://doi.org/10.5194/egusphere-2026-221
Preprint. Discussion started: 22 January 2026
© Author(s) 2026. CC BY 4.0 License.

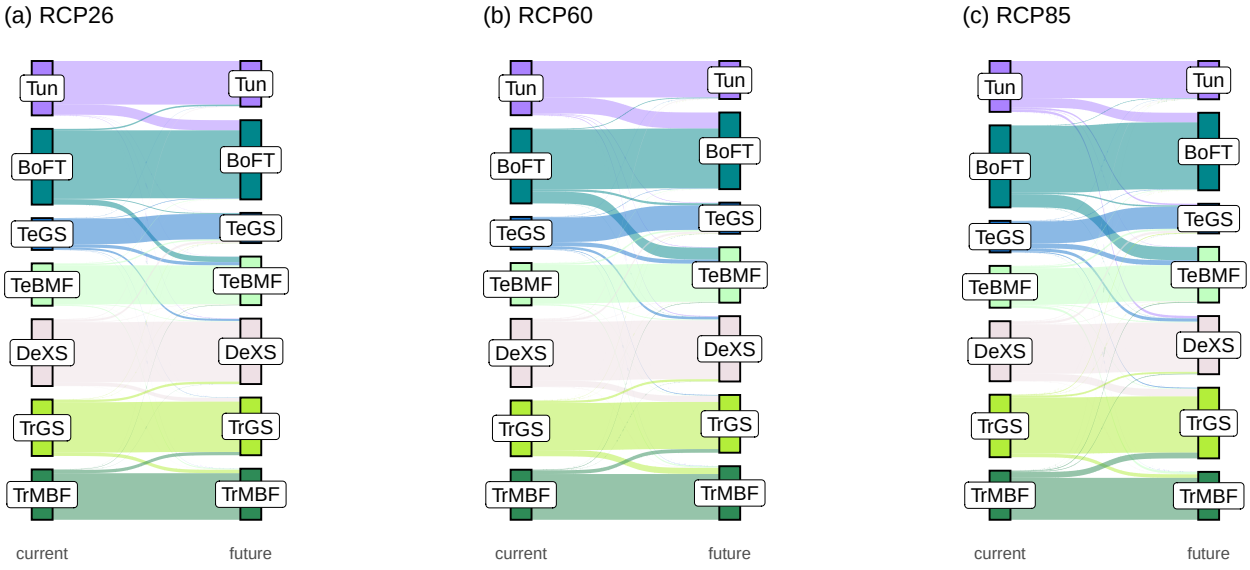

Figure 6. Biome change projected by GVMs for different RCPs. The Sankey diagrams illustrate transitions between different biomes between current and future conditions and biome classification informed by the Olson et al. (2001) map. For each scenario, all available GVMs were included. See Figs. S6, S7 for plots of individual models for RCP6.0. The height of the rectangles represents the biome coverage under current or future conditions, the width of the links represents the number of transitions between biomes. Here, we ignored biomes with low coverage, see supplementary Fig. S8 for graph with all biomes. See Fig. 4 or Table S7 for full biome names.